Published in final edited form as:
Cell Host Microbe. 2011 March 17; 9(3): 243–251. doi:10.1016/j.chom.2011.02.003.

A major role for capsule-independent phagocytosis-inhibitory mechanisms in mammalian infection by *Cryptococcus neoformans*

Cheryl D. Chun[+], **Jessica C. S. Brown**[+], and **Hiten D. Madhani**[*]
Dept. of Biochemistry and Biophysics, University of California, 600 16th St., San Francisco, CA 94158-2200

Summary

The anti-phagocytic polysaccharide capsule of the human fungal pathogen *Cryptococcus neoformans* is a major virulence attribute. However, previous studies of the pleiotropic virulence determinant Gat201, a GATA-family transcription factor, suggested that capsule-independent antiphagocytic mechanisms exist. We have determined that Gat201 controls the mRNA levels of ~1100 genes (16% of the genome) and binds the upstream regions of ~130 genes. Seven Gat201-bound genes encode for putative and known transcription factors—including two previously implicated in virulence—suggesting an extensive regulatory network. Systematic analysis pinpointed two critical Gat201-bound genes, *GAT204* (a transcription factor) and *BLP1*, which account for much of the capsule-independent antiphagocytic function of Gat201. A strong correlation was observed between the quantitative effects of single and double mutants on phagocytosis *in vitro* and on host colonization *in vivo*. This genetic dissection provides evidence that capsule-independent anti-phagocytic mechanisms are pivotal for successful mammalian infection by *C. neoformans*.

INTRODUCTION

The fungus *Cryptococcus neoformans* is a leading cause of morbidity and mortality in AIDS patients, resulting in one million cases and 600,000 deaths annually worldwide (Park et al., 2009). Although cryptococcosis is typically associated with immunodeficient patients, a recent outbreak caused by the sister species *Cryptococcus gattii* in the Pacific Northwest has resulted in the deaths of numerous immunocompetent individuals (Datta et al., 2009). It is thus critical to understand the interactions of the *Cryptococcus* species complex with the mammalian immune system.

C. neoformans is thought to be acquired through the inhalation of spores or yeast (Botts and Hull, 2010), and alveolar macrophages are considered the first line of defense against cryptococcal infection. Experimental evidence supports this, particularly early in infection (Monga, 1981; Osterholzer et al., 2009). *C. neoformans* can also survive and proliferate within the phagolysosome, as well as exit macrophages by lytic and nonlytic pathways, all

[*]hitenmadhani@gmail.com, tel (415) 514-0594, fax(415) 502-4315.
[+]These authors contributed equally to this work.

of which might be important for pathogenesis (Voelz and May, 2010). Macrophage activation has been shown to be important for T-cell proliferation, the development of the T-cell response, and chemokine-mediated recruitment of neutrophils and monocytes into the tissue (Monari et al., 2006a).

C. neoformans is rarely taken up by macrophages in the absence of opsonizing agents such as complement or antibodies, even after 24 hours of co-incubation (Levitz and DiBenedetto, 1989; Liu et al., 2008). This is in striking contrast to other yeasts: unopsonized *Saccharomyces cerevisiae* or *Candida albicans* are phagocytosed after less than an hour of co-incubation (Lohse and Johnson, 2008; Tejle et al., 2002). Opsonizing agents are likely present in lower levels early in infection. Within the lungs, complement is not present at constitutively high levels, but is synthesized in response to infection by many different cell types within the lungs and other tissues in a process that is estimated to take up to a week (Blackstock and Murphy, 1997; Rothman et al., 1989). Antibody generation is thought to take two to five weeks for peak production (Nussbaum et al., 1999). Therefore, cell-mediated killing by macrophages during the initial infection, prior to complement- and antibody-generation, is likely important for limiting proliferation of the invading pathogen. Studies have shown that AIDS patients generate less anti-*C. neoformans* antibody than healthy patients, and the severe prognosis for cryptococcosis in AIDS patients may be linked to this defect (Subramaniam et al., 2009). Antibodies generated by infected AIDS patients may be less protective against *C. neoformans* infection, produced at titers too low for effective opsonization, or production could be critically delayed early in infection (Dromer et al., 1988; Dromer et al., 1995). It is thus possible that yeast evasion of phagocytosis by macrophages plays an important role in the development of cryptococcosis in immunocompromised individuals.

The characteristic polysaccharide capsule of *C. neoformans* is considered one of its chief virulence traits. Its primary components are glucuronoxylomannan (GXM) and galactoxylomannan (GalXM), two high molecular mass polymers that have immunomodulatory properties, including suppression of both adaptive and innate immune mechanisms (Monari et al., 2006a; Monari et al., 2006b) The production of capsule by *C. neoformans* has been previously associated with inhibition of phagocytosis, although this correlation has been reported predominantly in the context of *C. neoformans* cells opsonized with serum (Del Poeta, 2004). It remains unclear how the capsular polysaccharides GXM and GalXM contribute to inhibition of unopsonized phagocytosis, which is presumably relevant to the control of disease early in the infection process. While the capsule is clearly an important virulence trait, clinical studies have suggested for decades the existence of important capsule-independent mechanisms: cryptococcosis cases produced by capsule-deficient strains exhibit a similar clinical course as infections produced by capsule-proficient strains (Torres et al., 2005).

Previously, our group described the first large-scale systematic genetic screen for virulence determinants of *C. neoformans* (Liu et al., 2008). We constructed and analyzed ~1200 gene knockout strains in the background of the H99 clinical isolate of *C. neoformans var grubii* (serotype A). A signature-tagged mutagenesis screen led to the identification of numerous factors required for the expression of known virulence factors as well as dozens of genes who contributed to virulence independently of known mechanisms. Among the mutants that produced the strongest defect in infectivity but did not affect proliferation rate at body temperature was a deletion in the *GAT201* gene (Liu et al., 2008). *GAT201* encodes a member of the GATA family of zinc finger transcriptional regulators that is conserved from yeast to man (Teakle and Gilmartin, 1998). A *GAT201* knockout mutant shows reduced capsule size and dramatic attenuation in virulence in a mouse inhalation model of infection. Significantly, we found that *gat201*Δ mutants are robustly taken up by macrophages in

unopsonized conditions. In contrast, less than 1% of macrophages are associated with yeast when infected with wild type *C. neoformans* for the same period. The defect in phagocytosis evasion by *gat201*Δ cells cannot be explained by the capsule size defect exhibited by *gat201*Δ cells: *cap10*Δ, *cap60*Δ, and *cap64*Δ cells, which are devoid of capsule, display a much more modest increase in association with macrophages than a *gat201*Δ mutant. More importantly, when *CAP* genes are knocked out in combination with *GAT201*, the resulting *cap*Δ*gat201*Δ strains still show dramatically increased percentages of macrophages with associated yeast cells over that displayed by the single *cap* mutants. These data suggested that Gat201 inhibits phagocytosis via both capsule-dependent and capsule-independent mechanisms (Liu et al., 2008). However, the relative contribution of these two functions to the virulence function of Gat201 remained to be addressed.

Given that Gat201 is predicted to be a transcriptional regulator, understanding its role in virulence requires identification and characterization of its direct targets. ChIP-chip and ChIP-seq are ideal methods for identifying direct targets of transcription factors, but the application of these methods to *C. neoformans* (whose polysaccharide capsule thickness can exceed the diameter of the cell) is nontrivial. In this study, we report the successful development of ChIP-chip methods for capsule-bearing *C. neoformans*, the identification of the direct targets of Gat201, and detailed analysis of these targets by systematic gene disruption and phenotypic characterization. We demonstrate that two targets, *GAT204* and *BLP1*, together explain a bulk of the capsule-independent phagocytosis evasion ("anti-phagocytosis") activity of Gat201, and that they are critical for *C. neoformans*'s ability to colonize the mammalian lung early in the infection process.

RESULTS

Gat201 controls the expression of ~1100 genes in response to environmental cues

Our previous work (Liu et al., 2008) indicated that Gat201 is a key virulence regulator, possibly through its inhibition of phagocytosis by macrophages. As Gat201 is a GATA-family transcription factor, we used microarray-based expression profiling to identify genes that are transcriptionally-regulated by Gat201 (Figure 1A). When we compared the transcript profiles of wild type cells to *gat201*Δ cells grown in standard yeast culture conditions (30°C, YPAD medium, atmospheric CO_2), we observed few changes in mRNA accumulation as determined using Statistical Analysis of Microarrays (SAM) analysis (Tusher et al., 2001). In comparison, when the strains were cultured in tissue culture conditions (37°C, DMEM, 5% CO_2), the same conditions used for culturing macrophages, we saw a dramatic Gat201-dependent transcriptional program (Figure 1B). Over 1,100 genes (~16% of the genome) showed a ≥2-fold difference in transcript levels and were identified by SAM analysis as differentially up- or down-regulated in a Gat201-dependent manner. We performed time course experiments utilizing RT-qPCR to examine gene expression of two representative genes from the up-regulated set (*MEU1* and *CNJ1810*) following transfer of cells from yeast to tissue culture conditions. Through the time course, we observed steady increases in transcript levels, with maximal expression occurring between 8 and 24 hours after transfer (Figure 1C). Interestingly, *GAT201* RNA levels also increased dramatically under these conditions, suggesting a positive feedback loop.

Gat201 binds the promoters of 126 genes and controls mRNA levels of 62 of these genes

To identify genes directly bound by Gat201, we used a chromatin immunoprecipitation-microarray hybridization (ChIP-chip) approach (Nobile et al., 2009). We tagged the endogenous *GAT201* gene with a C-terminal calmodulin-binding peptide-2X FLAG (CBP-2XFLAG) epitope. For these studies we developed a ChIP protocol for encapsulated cells (see Supplemental Procedures). Immunoprecipitated DNA (IP) and reference DNA

(WCE) from a Gat201-CBP-2XFLAG-expressing and an untagged parent strain were amplified and hybridized against a custom microarray spanning the entire genome of the strain H99. We identified 126 genes that show enrichment of Gat201-CBP-2XFLAG in their promoter regions when compared to the reference DNA and the untagged control strain (Figure 1D). As predicted from our time course analysis, Gat201-CBP-2XFLAG binds in the promoter of *GAT201* itself (Figure 1E).

Having identified genes with Gat201-CBP-2XFLAG bound in their promoters, we next sought to determine if their transcription was Gat201-dependent (Figure S1). We used RT-qPCR to quantify the mRNA levels for 126 genes with the strongest enrichment for Gat201-CBP-2XFLAG in their promoters, comparing wild type and *gat201*Δ cells grown in yeast culture and tissue culture conditions. Transcript levels were normalized to the levels found in wild type cells grown in yeast culture conditions. We identified a set of 62 Gat201-bound genes that demonstrated Gat201-dependent transcription induction in tissue culture conditions (Table 1). The promoter regions of these genes are enriched for a seven-nucleotide motif when compared to the promoters of all genes in the H99 *C. neoformans* genome (Figure S2A). Strikingly, Gat201 activates the transcription of genes encoding seven known and putative transcription factors: *CNBJ1500-A*, *GAT204*, *ECM2201*, *CIR1*, *LIV3*, *YLR236C02*, and *MET32*. These results suggest that Gat201 controls its remarkably large transcriptional regulon in part by activating the transcription of genes coding for downstream regulators (Figure 1F).

Identification of key Gat201-bound genes

We considered the 62 direct downstream targets of Gat201 to be likely effectors of Gat201-mediated phagocytosis inhibition. We thus targeted each of these genes for deletion by homologous recombination (Figure S1A). We successfully knocked out 46 of 62 genes, then tested each of the mutant strains for phagocytosis defects by co-incubation with RAW264.7 macrophages. Two genes emerged as having a role in phagocytosis inhibition: *CNAG_06346* and *CNAG_06762*. *CNAG_06346* encodes a protein with a highly conserved Barwin-like domain that we named Barwin-like protein 1 (Blp1). *CNAG_06762* encodes for the GATA-family transcription factor that we previously annotated as Gat204 (Chow et al., 2007). *BLP1* and *GAT204* show enhanced binding of Gat201-CBP-2XFLAG in their promoter regions (Figure S2B) and their expression is Gat201-dependent in tissue culture conditions (Figure 2A).

As Gat204 is itself a transcription factor, we examined *BLP1* transcription in *gat204* cells. *BLP1* expression is increased in *gat204* cells in tissue culture conditions (Figure 2B), suggesting that Gat204 may negatively regulate *BLP1* transcription, or that *BLP1* transcription is up-regulated as a compensatory mechanism when Gat204 is lost.

Gat201-bound genes mediate its anti-phagocytic function

Following 24 hour co-incubation with *blp1*Δ cells, approximately 2.5% of RAW264.7 macrophages were associated with yeast, a modest but statistically significant ($p<0.05$) increase over the 0.8% of macrophages associated with wild type yeast (Figure 2C). Co-incubation with *gat204*Δ cells resulted in yeast-association in ~9% of RAW264.7 cells. Strikingly, two independently-derived double knockout strains in *GAT204* and *BLP1* showed 25–30% of RAW264.7 macrophages associated with *C. neoformans*, indicating a functional synergy in their mechanism of phagocytosis inhibition, and recapitulating almost 40% of the original Gat201-dependent phenotype. We also observed this synergistic increase in phagocytosis in bone marrow-derived macrophages (BMDMs) (Figure S3A). Finally, we distinguished between macrophage-internalized and -externally associated yeast cells using differential staining techniques. We confirmed that the *gat204*Δ and *blp1*Δ

mutations acted synergistically to produce increases in actual uptake. We also documented an increase in external association of *gat204*Δ, *blp1*Δ, and *gat204*Δ*blp1*Δ strains (Figure S3B,C), which suggests that recognition and adherence may be what is triggering phagocytosis in the mutants.

Agrobacterium T-DNA insertion screen independently identifies *GAT201* and *GAT204*

Our original knockout library only covered a portion of the *C. neoformans* genome, so we sought a more global approach to identify anti-phagocytic factors. We therefore used the *Agrobacterium tumefaciens* T-DNA system (McClelland et al., 2005) to produce insertional mutants across the *C. neoformans* genome and then screened this mutant library for anti-phagocytosic defects (Figure S1B). A library of ~30,000 insertions was generated, from which 2×10^8 yeast cells from overnight YPAD culture were added to plated RAW264.7 macrophages. Following rounds of selection for phagocytosed yeast cells, the yeast culture was enriched for strains mutated in genes important for phagocytosis inhibition. The sites of insertion were mapped for strains that individually demonstrated increased uptake by macrophages. Strikingly, this global approach identified three independent insertional events each into *GAT201* and *GAT204* (Figure S1C). We also identified the copper transporter *CTR2*, a gene not regulated by Gat201 that causes capsule defects when mutated and is thus presented elsewhere (Chun and Madhani, 2010). We did not identify strains with mutations in *BLP1* in this screen, which is not surprising given the mild phenotype of the *blp1*Δ single mutant. We also did not identify capsule gene mutants; however, these strains exhibit a growth defect (Chun and Madhani, unpublished observation) and are likely out-competed during the selection process. Another gene known to be involved in capsule-independent phagocytosis, *APP1*, acts only in opsonized cells (Luberto et al., 2003), and was not identified in our screen for unopsonized phagocytosis. These data underline the importance of Gat201 and Gat204 in limiting phagocytosis of *C. neoformans*.

Gat204 and Blp1 are dispensable for capsule formation

Interestingly, the level of capsule, as detected by India ink staining (Figure 2D), was unchanged in these mutants, unlike in the *gat201*Δ strain (Liu et al., 2008). *gat204*Δ, *blp1*Δ, and *gat204*Δ*blp1*Δ mutants were also stained for β-glucan, chitin, and mannoprotein but did not show any changes relative to wild-type cells (data not shown), demonstrating that gross cell surface architecture is unchanged in these mutants. Growth at 37°C was unchanged in the *gat204*Δ and *blp1*Δ mutant strains (Figure 3A). None of the mutants were deficient in the production of melanin, a pigmented compound thought to be important for virulence in the host (Figure 3B).

Blp1 is part of a six-gene family in *C. neoformans*

SMART protein sequence analysis of Blp1 identified a conserved Barwin-like domain (Figure S2C). This domain is found in a number of protein families in plants, fungi, and bacteria, several members of which have antifungal properties (Hejgaard et al., 1992). Analysis of predicted protein sequence by SignalP reveals a high probability (1.000) of a signal peptide. *BLP1* appears to be part of a six-member family in *C. neoformans*, all of which contain the Barwin-like domain and a signal sequence.

Inhibition of phagocytosis correlates with effective colonization of the lungs

To determine whether inhibition of phagocytosis by *C. neoformans* correlates with its ability to colonize the lung, we performed competitive infections. Wild type cells were mixed in equal proportion with *gat201*Δ, *gat204*Δ, *blp1*Δ, or *gat204*Δ*blp1*Δ cells. As a control strain, we used a knockout mutant in *SXI1*, which is not expressed in non-mating cells and is dispensable for virulence (Hull et al., 2004). Inocula were administered to mice through an

inhalation model of infection. The lungs were harvested after three or ten days and the proportion of mutant to wild type cells assessed. Strikingly, we observed a correlation between the degree of phagocytosis inhibition in a given strain and the relative ability of that strain to colonize the lung tissue (Figure 3C). While the mutant cells made up ~50% of each inoculum, their prevalence after three or ten days in the lungs correlated with their anti-phagocytic abilities. The *gat201*Δ strain, which showed the least phagocytic inhibition of all the strains tested, was entirely absent from lung tissue homogenate-derived colonies. The *gat204*Δ strain, which showed decreased phagocytic inhibition compared to wild type, also displayed decreased representation in the lungs (~27% at 3dpi, ~19% at 10dpi). *gat204*Δ*blp1*Δ, which displayed a level of phagocytic inhibition between that of *gat201*Δ and *gat204*Δ, showed a level of representation in the lungs also intermediate to the two strains. The *blp1*Δ mutant, which displayed the weakest phagocytosis phenotype, and the control *sxi1*Δ mutant represented ~50% of the cells recovered from the lungs.

DISCUSSION

Cryptococcus species produce a polysaccharide capsule, which numerous studies have shown to be a major virulence factor and an important mechanism of immune modulation. In particular, capsule inhibits phagocytosis of *C. neoformans* by macrophages (Monari et al., 2006a). However, our previous work demonstrates that the pleiotropic transcriptional activator Gat201 controls a capsule-independent mechanism by which *C. neoformans* evades phagocytosis but also regulates capsule synthesis (Liu et al., 2008). Here, we describe a regulatory circuit dissection approach to further illuminate capsule-independent antiphagocytic mechanisms and to test their roles in infection. The work described in this paper demonstrates that at least two such mechanisms exist, begins to identify potential end-effectors of this regulatory circuit, and—importantly—provides strong evidence that such mechanisms are important for successful mammalian infection by *C. neoformans*.

An integrative approach identifies the direct targets of the Gat201 virulence regulator

We found that over one thousand genes, or approximately 1/6 of the *C. neoformans* genome, showed statistically significant changes in expression in *gat201*Δ cells compared to wild type. As expression of *GAT201* itself was induced in these conditions, Gat201 could function downstream of a signaling pathway(s) that senses environmental changes and modulates a massive reprogramming of the cellular transcriptome.

To identify the direct targets of Gat201, we developed ChIP-chip methods. Through this approach we identified 126 genes that demonstrate robust binding of Gat201 in their promoter regions, 62 of which depend on Gat201 for transcript accumulation in tissue culture conditions. Significantly, seven targets of Gat201 themselves encode known or predicted transcription factors, two of which, Liv3 and Cir1, have been previously implicated in pathogenicity (Jung et al., 2006; Liu et al., 2008). The results reported here implicate Gat204 in infectivity. Thus, it appears that Gat201 is part of a critical large virulence transcriptional regulatory network that controls pathogenicity in response to environmental signals.

Systematic analysis reveals the existence of multiple capsule-independent anti-phagocytosis mechanisms

Through a systematic gene disruption approach, we identified two genes, *BLP1* and *GAT204*, which affect the ability of *C. neoformans* to evade unopsonized phagocytosis by macrophages. Together, these two genes recapitulate a significant portion of the phenotype of the *gat201*Δ mutant strain. These observations suggest that at least three mechanisms

exist to inhibit phagocytosis: GXM, those dependent on Blp1 and Gat204, and at least one mechanism that is Gat201-dependent but Blp1/Gat204-independent.

Capsule-independent phagocytosis inhibition and mammalian infectivity of *Cryptococcus neoformans*

Finally, we have demonstrated that the relative ability of a given strain to evade or inhibit phagocytosis correlates with its ability to survive and proliferate within the lung tissue. We examined time points relatively early in infection, when we expect alveolar macrophages to play a crucial role in the initial host response, but before a full adaptive immune response develops. Cells lacking Gat201 are cleared from the lungs of infected mice within three days, demonstrating an early and pivotal role for this transcription factor in pathogen success. Significantly, the analysis of single and double mutants demonstrated that the roles of Gat201, Gat204 and Blp1 in survival within the murine lung are proportional to their impact on phagocytosis *in vitro*. The correlation between the *in vitro* and *in vivo* data strongly indicates that multiple capsule-independent anti-phagocytosis mechanisms are critical for infection of the mammalian host. Thus, while a major focus of *C. neoformans* research has justifiably been its polysaccharide capsule, this work demonstrates capsule-independent anti-phagocytic mechanisms are important for successful host colonization.

EXPERIMENTAL PROCEDURES

Gene nomenclature

Genes were identified using annotation from the H99 sequence from the Broad Institute (http://www.broadinstitute.org/annotation/genome/cryptococcus_neoformans/MultiHome.html) and from our own annotation of the H99 sequence (http://cryptogenome.ucsf.edu). Gene annotations from the Broad are designated by their nomenclature “CNAG_#”, while our own annotations are designated “CDS_#”.

Strains and media

C. neoformans growth conditions were as previously described (Chun et al., 2007; Chun and Madhani, 2010; Liu et al., 2008), with minor modifications found in the Supplemental Procedures.

Phagocytois assay

RAW264.7 macrophage assays were performed as previously described (Chun and Madhani, 2010; Liu et al., 2008). Bone marrow-derived macrophage experiments were performed in much the same manner with minor modifications described in Supplemental Procedures.

Expression profiling

Expression profiling was performed as previously described (Liu et al., 2008) with minor modifications described in Supplemental Procedures. Analysis was performed as described in Chun et al., 2007.

ChIP-on-chip

The ChIP-chip tiling arrays were designed on 244,000 probes of 60-bp length, averaging 80-bp between probes, across the entire H99 sequence as it was published by the Broad Institute, current to 2007. Experiments were performed as previously described (Nobile et al., 2009) with *C. neoformans*-specific modifications described in the Supplemental Procedures.

RT-qPCR

Gene expression differences observed using microarray-based transcript profiling were confirmed utilizing RT-qPCR as previously described (Chun et al., 2007) with minor modifications (see Supplemental Procedures).

A. tumefaciens-mediated transformation of *C. neoformans*

These experiments were performed as described in McClelland et al., 2005 (McClelland et al., 2005) with minor modifications as described in Chun and Madhani, 2010.

Phagocytosis Screen with Insertional Mutant Library

This procedure was performed as previously described (Chun and Madhani, 2010).

Capsule assay

Experiments were performed as previously described (Liu et al., 2008). See Supplemental Procedures for more details.

Growth curve

Overnight YPAD cultures grown at 37°C were diluted back to OD_{600}=0.1 in YPAD, in triplicate. Cultures were grown at 37°C for 7 hours, and the OD_{600} was measured every 2–3 hours.

Melanin assay

From overnight culture, *C. neoformans* cells were diluted to OD_{600} = 0.6 in water then spotted onto melanin-inducing plates containing L-DOPA (L-dihydroxyphenylalanine, Sigma, 100 mg l^{-1}) and grown for three days at 37°C.

Intranasal co-infection experiments

Experiments were performed as described previously (Liu et al., 2008).

Supplementary Material

Refer to Web version on PubMed Central for supplementary material.

Acknowledgments

We thank Paolo Manzanillo and Jeffery S. Cox for the kind gift of bone marrow-derived macrophages. This work was supported by grant R01AI065519 from the National Institute of Allergy and Infectious Disease (NIAID) to HDM. CDC and JCSB are supported by NIAID grant 5T32AI060537-07 to the UCSF Microbial Pathogenesis Program.

References

Blackstock R, Murphy JW. Secretion of the C3 component of complement by peritoneal cells cultured with encapsulated Cryptococcus neoformans. Infect Immun. 1997; 65:4114–4121. [PubMed: 9317016]

Botts MR, Hull CM. Dueling in the lung: how Cryptococcus spores race the host for survival. Curr Opin Microbiol. 2010; 13:437–442. [PubMed: 20570552]

Chow ED, Liu OW, O'Brien S, Madhani HD. Exploration of whole-genome responses of the human AIDS-associated yeast pathogen Cryptococcus neoformans var grubii: nitric oxide stress and body temperature. Curr Genet. 2007; 52:137–148. [PubMed: 17661046]

Chun CD, Liu OW, Madhani HD. A link between virulence and homeostatic responses to hypoxia during infection by the human fungal pathogen Cryptococcus neoformans. PLoS Pathog. 2007; 3:e22. [PubMed: 17319742]

Chun CD, Madhani HD. Ctr2 links copper homeostasis to polysaccharide capsule formation and phagocytosis inhibition in the human fungal pathogen Cryptococcus neoformans. PLoS One. 2010:5.

Datta K, Bartlett KH, Baer R, Byrnes E, Galanis E, Heitman J, Hoang L, Leslie MJ, MacDougall L, Magill SS, et al. Spread of Cryptococcus gattii into Pacific Northwest region of the United States. Emerg Infect Dis. 2009; 15:1185–1191. [PubMed: 19757550]

Del Poeta M. Role of phagocytosis in the virulence of Cryptococcus neoformans. Eukaryot Cell. 2004; 3:1067–1075. [PubMed: 15470235]

Dromer F, Aucouturier P, Clauvel JP, Saimot G, Yeni P. Cryptococcus neoformans antibody levels in patients with AIDS. Scand J Infect Dis. 1988; 20:283–285. [PubMed: 3043650]

Dromer F, Denning DW, Stevens DA, Noble SM, Hamilton JR. Anti-Cryptococcus neoformans antibodies during cryptococcoss in patients with acquired immunodeficiency syndrome. Serodiagnosis and Immunotherapy in Infectious Disease. 1995; 7:181–188.

Hejgaard J, Jacobsen S, Bjorn SE, Kragh KM. Antifungal activity of chitin-binding PR-4 type proteins from barley grain and stressed leaf. FEBS Lett. 1992; 307:389–392. [PubMed: 1644196]

Hull CM, Cox GM, Heitman J. The alpha-specific cell identity factor Sxi1alpha is not required for virulence of Cryptococcus neoformans. Infect Immun. 2004; 72:3643–3645. [PubMed: 15155676]

Jung WH, Sham A, White R, Kronstad JW. Iron regulation of the major virulence factors in the AIDS-associated pathogen Cryptococcus neoformans. PLoS Biol. 2006; 4:e410. [PubMed: 17121456]

Levitz SM, DiBenedetto DJ. Paradoxical role of capsule in murine bronchoalveolar macrophage-mediated killing of Cryptococcus neoformans. J Immunol. 1989; 142:659–665. [PubMed: 2521352]

Liu OW, Chun CD, Chow ED, Chen C, Madhani HD, Noble SM. Systematic genetic analysis of virulence in the human fungal pathogen Cryptococcus neoformans. Cell. 2008; 135:174–188. [PubMed: 18854164]

Lohse MB, Johnson AD. Differential phagocytosis of white versus opaque Candida albicans by Drosophila and mouse phagocytes. PLoS One. 2008; 3:e1473. [PubMed: 18213381]

Luberto C, Martinez-Marino B, Taraskiewicz D, Bolanos B, Chitano P, Toffaletti DL, Cox GM, Perfect JR, Hannun YA, Balish E, et al. Identification of App1 as a regulator of phagocytosis and virulence of Cryptococcus neoformans. J Clin Invest. 2003; 112:1080–1094. [PubMed: 14523045]

McClelland CM, Chang YC, Kwon-Chung KJ. High frequency transformation of Cryptococcus neoformans and Cryptococcus gattii by Agrobacterium tumefaciens. Fungal Genetics and Biology. 2005; 42:904–913. [PubMed: 16260158]

Monari C, Bistoni F, Vecchiarelli A. Glucuronoxylomannan exhibits potent immunosuppressive properties. FEMS Yeast Res. 2006a; 6:537–542. [PubMed: 16696649]

Monari C, Kozel TR, Paganelli F, Pericolini E, Perito S, Bistoni F, Casadevall A, Vecchiarelli A. Microbial immune suppression mediated by direct engagement of inhibitory Fc receptor. J Immunol. 2006b; 177:6842–6851. [PubMed: 17082598]

Monga DP. Role of macrophages in resistance of mice to experimental cryptococcosis. Infect Immun. 1981; 32:975–978. [PubMed: 6265377]

Nobile CJ, Nett JE, Hernday AD, Homann OR, Deneault JS, Nantel A, Andes DR, Johnson AD, Mitchell AP. Biofilm matrix regulation by Candida albicans Zap1. PLoS Biol. 2009; 7:e1000133. [PubMed: 19529758]

Nussbaum G, Anandasabapathy S, Mukherjee J, Fan M, Casadevall A, Scharff MD. Molecular and idiotypic analyses of the antibody response to Cryptococcus neoformans glucuronoxylomannan-protein conjugate vaccine in autoimmune and nonautoimmune mice. Infect Immun. 1999; 67:4469–4476. [PubMed: 10456888]

Osterholzer JJ, Milam JE, Chen GH, Toews GB, Huffnagle GB, Olszewski MA. Role of dendritic cells and alveolar macrophages in regulating early host defense against pulmonary infection with Cryptococcus neoformans. Infect Immun. 2009; 77:3749–3758. [PubMed: 19564388]

Park BJ, Wannemuehler KA, Marston BJ, Govender N, Pappas PG, Chiller TM. Estimation of the current global burden of cryptococcal meningitis among persons living with HIV/AIDS. AIDS. 2009; 23:525–530. [PubMed: 19182676]

Rothman BL, Merrow M, Despins A, Kennedy T, Kreutzer DL. Effect of lipopolysaccharide on C3 and C5 production by human lung cells. J Immunol. 1989; 143:196–202. [PubMed: 2732467]

Subramaniam K, Metzger B, Hanau LH, Guh A, Rucker L, Badri S, Pirofski LA. IgM(+) memory B cell expression predicts HIV-associated cryptococcosis status. J Infect Dis. 2009; 200:244–251. [PubMed: 19527168]

Teakle GR, Gilmartin PM. Two forms of type IV zinc-finger motif and their kingdom-specific distribution between the flora, fauna and fungi. Trends Biochem Sci. 1998; 23:100–102. [PubMed: 9581501]

Tejle K, Magnusson KE, Rasmusson B. Phagocytosis and phagosome maturation are regulated by calcium in J774 macrophages interacting with unopsonized prey. Biosci Rep. 2002; 22:529–540. [PubMed: 12635850]

Torres HA, Prieto VG, Raad II, Kontoyiannis DP. Proven pulmonary cryptococcosis due to capsule-deficient Cryptococcus neoformans does not differ clinically from proven pulmonary cryptococcosis due to capsule-intact Cr. neoformans. Mycoses. 2005; 48:21–24. [PubMed: 15679661]

Tusher VG, Tibshirani R, Chu G. Significance analysis of microarrays applied to the ionizing radiation response. Proc Natl Acad Sci U S A. 2001; 98:5116–5121. [PubMed: 11309499]

Voelz K, May RC. Cryptococcal Interactions with the Host Immune System. Eukaryot Cell. 2010; 9:835–846. [PubMed: 20382758]

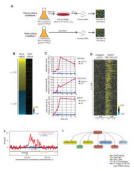

Figure 1. Identification of Gat201 transcriptional program and direct Gat201 targets

(A) Schematic of growth conditions used for transcriptional microarrays of yeast cells grown in tissue culture conditions (DMEM, 37°C, 5% CO_2) or yeast culture conditions (YPAD, 30°C, atmospheric CO_2).

(B) Transcript profiling using custom whole-genome DNA microarrays was performed comparing *gat201*Δ versus wild type cells grown in tissue culture and in yeast culture conditions. Genes shown are those with both a minimum of a two-fold change and a statistically significant difference (using SAM analysis) between expression profiles in tissue culture and yeast media conditions. Values are plotted as the average ratio of transcript level in *gat201*Δ cells vs. wild type cells (log_2) from four arrays per growth condition.

(C) RT-qPCR analysis of the indicated transcripts following transfer from yeast culture conditions into tissue culture conditions. Samples were harvested at the indicated time points following transfer for RNA isolation and cDNA synthesis. Error bars at the 24 hour time point are the standard deviation of two samples.

(D) Global summary of ChIP-chip results. Genes with enriched for Gat201-CBP-2XFLAG bound in their promoter regions were identified by comparing signals from replicate experiments performed with untagged and tagged strains. Genes are displayed which the largest difference between tagged and untagged genotypes in median value of the top five probe values among those within 1 kb of the predicted translational start site. Depicted are the ratios (log_2) of immunoprecipitated DNA (IP) to whole cell extract (WSE) for each probe.

(E) Example of ChIP-chip data. Ratios (log_2) of IP DNA to WCE were plotted for each probe of the two tiling arrays at the chromosomal coordinates indicated. Asterisks indicated locations of motif in the chromosomal sequence shown.

(F) Gat201 directly binds the regulatory regions of set of known and putative transcription factors.

See also Figure S2.

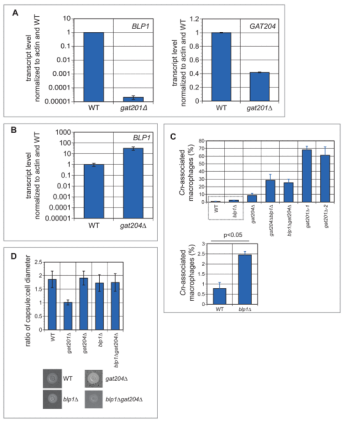

Figure 2. *In vitro* analysis of Gat204 and Blp1

(A) Activation of *BLP1* and *GAT204* by Gat201. *BLP1* (left panel) and *GAT204* (right panel) transcript levels were assessed in wild type and *gat201*Δ cells grown in tissue culture conditions for 24 hours. Error bars are standard deviation (SD) of 2–4 samples.

(B) Repression of *BLP1* by Gat204. *BLP1* transcript levels were assessed in wild type and *gat204*Δ cells grown in tissue culture conditions for 24 hours. Error bars are SD of two samples.

(C) Quantification of phagocytosis defects. RAW264.7 macrophages were co-incubated with the designated *C. neoformans* strains for 24 hours then washed three times with PBS to remove unphagocytosed yeast. The macrophages were then counted to assay the number of macrophages with yeast associated. At least 200 macrophages were counted per well and each strain was assayed in triplicate. By Student's t-test, the difference between *blp1*Δ and wild type association with macrophages was determined to be statistically significant.

(D) Quantitative measurements of capsule size. Capsule was induced in the indicated strains by incubation in tissue culture conditions for 24 hours. Capsule and cell size were measured for at least 30 cells per strain, and the ratio of capsule to cell diameter calculated and averaged for each strain. Error bars denote SD.

See also Figure S1.

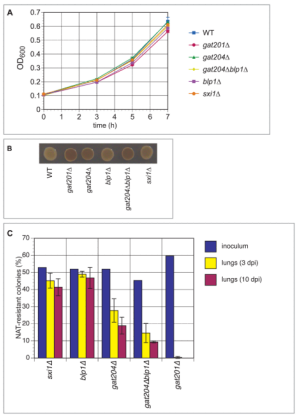

Figure 3. Anti-phagocytosis mutants show reduced fitness during infection but normal rates in vitro

(A) Growth rate measurements. Log-phase wild type and mutant strains were grown for seven hours at 37°C in YPAD medium, and OD_{600} was measured every 2–3 hours. Error bars denote SD for cultures grown in triplicate.

(B) Melanin assays. Melanin assay on L-DOPA plates demonstrates that none of the strains are hypomelanized. *gat201*Δ is hypermelanized, as previously noted in Liu et al (2008). *gat204*Δ is also hypermelanized, as is the *gat204*Δ*blp1*Δ mutant.

(C) Mouse infection data. Approximately 1:1 mixtures of H99 and the indicated mutant (marked with a nourseothricin [NAT] resistance gene) were inoculated intranasally into mice (A/J) (5×10^5 total cells/mouse). The actual proportion of mutant cells in each inoculum were determined by plating a dilution of the inoculum on non-selective medium and then assaying 100–200 individual colonies for NAT resistance. At three and ten days post-infection, animals were sacrificed and the lungs, brains, and spleen from each were homogenized and serial dilutions were plated. 100–200 colonies per organ were assayed for NAT resistance to determine the percentage of mutant cells. Error bars represent the SD from three mice per inoculum. See also Figure S3.

Table 1

Gat201 target genes

Genes with Gat201-CBP-2XFLAG bound in their promoter with Gat201-dependent induction in tissue culture conditions. CNAG numbers are gene identifiers from the Broad Institute's annotation of H99. CDS numbers are gene identifiers from our annotation. "WT/*gat201*Δ" refers to the ratio of transcript level for a given gene in wild type cells over that in *gat201*Δ cells in tissue culture conditions. "DMEM induction" is the amount of transcript for a given gene in wild type cells grown in tissue culture conditions relative to the transcript level in wild type cells grown in yeast culture conditions. When previously characterized in the literature, the name for a gene is given. If there is no prior reference to the gene, the name assigned in our annotation is given, if available. Annotations were assigned by BLASTP and SMART analysis. Italics indicate those genes that were not successfully knocked out

CNAG #	CDS #	*gat201*Δ/WT	DMEM Induction	Name	Annotation
CNAG_06517	CDS_4922	144.51	117.50	YOR296W02	C2 domain-containing protein
CNAG_04736	CDS_5892	103.76	153.95	CNJ1800	unknown
CNAG_06186	CDS_1099	37.53	103.95	CNM1740	sugar transport
CNAG_01553	CDS_3244	35.87	36.20	CNC0890	CHORD-containing protein
CNAG_05867	CDS_3724	32.25	239.48	CNF3650	fucose permease
CNAG_01601	*CDS_2811*	*31.95*	*195.53*	*ATG15*	*potential vacuolar triglyceride lipase*
CNAG_06389	CDS_7034	31.10	20.86		unknown
CNAG_05147	CDS_5668	23.64	51.11	CNI2090	unknown
CNAG_04735	CDS_5889	23.00	69.96	CNJ1810	metalloprotease
CNAG_00165	CDS_4036	18.59	39.71	MEU1	phosphorylase
CNAG_04756	CDS_5770	15.69	72.05	CNJ1610	ribonuclease H-related protein
CNAG_00331	*CDS_4152*	*8.49*	*22.77*	*YMR210W01*	*alpha/beta hydrolase fold*
CNAG_02553	*CDS_1762*	*8.31*	*17.90*	*SPS1904*	*putative oxidoreductase*
CNAG_05821	*ND*	*8.20*	*20.59*		*unknown*
CNAG_03848	CDS_6469	8.07	22.97	CNB2310-B	putative glutaredoxin
CNAG_05312	CDS_5280	7.93	3.45	CNI3590	macrophage activating glycoprotein
CNAG_00456	*ND*	*6.93*	*24.06*		*unknown*
CNAG_00374	CDS_6603	6.27	10.73		unknown
CNAG_01777	CDS_2931	6.19	1.47	YNL274C03	Glyoxylate reductase/
CNAG_00919	*CDS_669*	*5.67*	*3.05*	*KEX101*	*carboxypeptidase S3*
CNAG_06762	CDS_5944	5.57	36.16	GAT204	GATA-family transcription factor

CNAG #	CDS #	*gat201*Δ/WT	DMEM Induction	Name	Annotation
CNAG_01552	*CDS_3426*	*5.38*	*44.66*	*BET1*	*T-SNARE membrane protein*
CNAG_06346	ND	5.04	5.14	BLP1	Barwin-like domain
CNAG_05640	CDS_5612	5.02	7.19	SMF1	NRAMP manganese transporter
CNAG_06493	CDS_4944	4.81	14.99	CNN2220	unknown
CNAG_02189	CDS_1614	4.68	7.46	YJL216C	putative alpha-amylase
CNAG_03012	*CDS_2777*	*4.52*	*2.07*	*QSP1*	*quorum sensing peptide*
CNAG_02777	CDS_3007	4.49	158.67	PHO840	putative phosphate transporter
CNAG_05664	CDS_5254	2.17	1.22	BAT1	branched amino-acid transaminase
CNAG_03136	CDS_2688	4.29	20.43	CNG0410	putative fatty acid synthase
CNAG_04768	*CDS_5907*	*4.14*	*6.35*	*CNBJ1500-A*	*Gal4-like DNA binding domain*
CNAG_06098	CDS_1286	4.09	5.40	CNM0910	glucosamine-6-phosphate
CNAG_03122	ND	3.82	772.37		unknown
CNAG_06200	CDS_1088	3.70	3.92	CNM1860	PAS domain-containing protein
CNAG_06242	CDS_1107	3.56	8.20	CFT1	high-affinity iron permease
CNAG_06108	ND	3.40	2.83		unknown
CNAG_01778	*CDS_3364*	*3.30*	*6.15*	*CNC4450*	*mitochondrial carrier protein-like*
CNAG_04737	CDS_5893	3.25	1.50	CNJ1790	potential methyltransferase
CNAG_04517	ND	3.21	3.64		unknown
CNAG_00883	CDS_781	3.00	11.16	ECM2201	Gal4-like DNA binding
CNAG_05229	CDS_5329	2.86	19.11	CNI2770	stomatin-like protein
CNAG_00884	CDS_775	2.74	5.74	SEC10	unknown
CNAG_03413	CDS_2415	2.73	9.52	CNG3070	alginate lyase
CNAG_04312	*CDS_112*	*2.43*	*2.88*	*PMI4001*	*mannose-6-phosphate isomerase*
CNAG_05835	CDS_3521	2.35	3.21	LIV3	Wor1-like transcription factor
CNAG_03915	CDS_6280	2.32	9.78	CNB1700	unknown
CNAG_04140	CDS_43	2.20	4.99	CNH2650	unknown
CNAG_02856	*CDS_3358*	*2.20*	*2.05*	*TRK1*	*putative potassium transporter*
CNAG_03412	CDS_2417	2.16	3.97	CTS202	chitinase
CNAG_02219	CDS_1876	2.08	1.71	YLR247C02	zinc finger

CNAG #	CDS #	*gat201Δ/WT*	DMEM Induction	Name	Annotation
CNAG_03847	CDS_6346	2.08	7.85	CNB2320	unknown
CNAG_01681	CDS_2877	2.07	10.13	FCY2201	putative purine-cytosine permease
CNAG_06763	CDS_5942	2.05	6.61	DIA4	putative seryl-tRNA synthetase
CNAG_04864	CDS_5991	2.01	3.22	CIR1	GATA-type transcription factor
CNAG_04436	CDS_146	1.99	12.71	CNH1150	unknown
CNAG_04435	*ND*	*1.97*	*6.83*		*ferric reductase*
CNAG_00184	CDS_4067	1.84	1.87	PCF11	Pre-mRNA cleavage complex II
CNAG_00068	CDS_4631	1.81	7.46	MET32	Zn C2H2-domain containing protein
CNAG_06187	ND	2.54	3.39	STR1	streptomycin biosynthesis protein
CNAG_01040	CDS_703	24.63	10.64	KEX102	carboxypeptidase S3
CNAG_05159	*ND*	*18.83*	*6.09*		*unknown*
CNAG_00546	*CDS_4340*	*2.95*	*5.68*	*CHS301*	*chitin synthase*